Metabolomics analysis in rat hearts with ischemia/reperfusion injury after diazoxide postconditioning

Cen Xiang[1,2†], Shoujia Yu[1†], Qiyang Ren[1], Boyi Jiang[2], Jing Li[1], Donghang Zhang[3] and Yiyong Wei[4]*

[1]Department of Anesthesiology, Affiliated Hospital of Zunyi Medical University, Zunyi, China, [2]Department of Anesthesiology, Zhuhai Hospital of Integrated Traditional Chinese and Western Medicine, Zhuhai, China, [3]Department of Anesthesiology, West China Hospital of Sichuan University, Chengdu, China, [4]Department of Anesthesiology, Longgang District Maternity and Child Healthcare Hospital of Shenzhen City (Longgang Maternity and Child Institute of Shantou University Medical College), Shenzhen, China

Background: Diazoxide is a selective mitochondrial-sensitive potassium channel opening agent that has a definite effect on reducing myocardial ischemia/reperfusion injury (MIRI). However, the exact effects of diazoxide postconditioning on the myocardial metabolome remain unclear, which might contribute to the cardioprotective effects of diazoxide postconditioning.

Methods: Rat hearts subjected to Langendorff perfusion were randomly assigned to the normal (Nor) group, ischemia/reperfusion (I/R) group, diazoxide (DZ) group and 5-hydroxydecanoic acid + diazoxide (5-HD + DZ) group. The heart rate (HR), left ventricular developed pressure (LVDP), left ventricular end-diastolic pressure (LVEDP), and maximum left ventricular pressure (+dp/dtmax) were recorded. The mitochondrial Flameng scores were analysed according to the ultrastructure of the ventricular myocardial tissue in the electron microscopy images. Rat hearts of each group were used to investigate the possible metabolic changes relevant to MIRI and diazoxide postconditioning.

Results: The cardiac function indices in the Nor group were better than those in the other groups at the end point of reperfusion, and the HR, LVDP and $+dp/dt_{max}$ of the Nor group at T2 were significantly higher than those of the other groups. Diazoxide postconditioning significantly improved cardiac function after ischaemic injury, and the HR, LVDP and $+dp/dt_{max}$ of the DZ group at T2 were significantly higher than those of the I/R group, which could be abolished by 5-HD. The HR, LVDP and $+dp/dt_{max}$ of the 5-HD + DZ group at T2 were significantly lower than those of the DZ group. The myocardial tissue in the Nor group was mostly intact, while it exhibited considerable damage in the I/R group. The ultrastructural integrity of the myocardium in the DZ group was higher than that in the I/R and 5-HD + DZ groups. The mitochondrial Flameng score in the Nor group was lower than that in the I/R, DZ and 5-HD + DZ groups. The mitochondrial Flameng score in the DZ group was lower than that in the I/R and 5-HD + DZ groups. Five metabolites, namely, L-glutamic acid, L-threonine, citric acid, succinate, and nicotinic acid, were suggested to be associated with the protective effects of diazoxide postconditioning on MIRI.

Conclusion: Diazoxide postconditioning may improve MIRI via certain metabolic changes. This study provides resource data for future studies on metabolism relevant to diazoxide postconditioning and MIRI.

Introduction

Myocardial ischemia/reperfusion injury (MIRI) refers to a series of complex pathophysiological changes in the myocardium after ischemia, hypoxia and blood perfusion, which can result in severe and even irreversible myocardial damage (Russo et al., 2017). MIRI is a serious threat to human health. Mitochondrial ATP-sensitive potassium channels (mitoKATP) are located in the mitochondrial intima and are considered end-effectors for alleviating MIRI (Mironova et al., 2019). Diazoxide is a specific opener of the mitoKATP channel. Studies have found that diazoxide can attenuate MIRI (Onukwufor et al., 2016; Jin et al., 2020; Chen et al., 2021). However, the exact modulation mechanism for alleviating MIRI has not been clearly illustrated.

Energy metabolism dysfunction is one of the main pathological changes during MIRI (Kolwicz et al., 2013). Hypoxia inhibits the oxidative metabolism of fatty acids, glucose, and amino acids and activates anaerobic glycolysis (Zuurbier et al., 2020). These metabolic changes largely determine the actual damage that occurs to the heart following ischemia/reperfusion. Pan et al. (2020) applied proteomic techniques to find that diazoxide postconditioning could upregulate three proteins, namely, NADH dehydrogenase (ubiquinone) flavoprotein 1 (NDUFA1), NADH-ubiquinone oxidoreductase 75 kDa subunit (NDUFS1) and 2-oxoglutarate dehydrogenase (OGDH), which are involved in maintaining mitochondrial respiratory chain function and regulating the tricarboxylic acid (TCA) cycle to maintain normal energy supply. Furthermore, mitoKATP channel opening regulates the expression of some genes (*Mt-nd6, Idh2,* and *Acadl*) related to energy metabolism and regulates the TCA cycle and fatty acid metabolism to promote ATP production (Cao et al., 2015). Therefore, mitoKATP channel opening may be involved in regulating cardiac metabolism and maintaining the balance of energy demand and supply during MIRI. However, the metabolic changes related to MIRI and diazoxide postconditioning were not well determined.

In the present study, we hypothesized that diazoxide postconditioning can impact principal metabolic pathways in hearts with MIRI. This study may provide new insights into the protective mechanism of diazoxide postconditioning in heart MIRI.

Materials and methods

Animals. Twenty-four male Sprague-Dawley (SD) rats (250–300 g, 16–20 weeks old) were housed in a specific pathogen-free (SPF) animal facility with 12-h light/dark cycles and *ad libitum* access to food and water. All experimental procedures were approved by the Animal Care and Use Committee of Zunyi Medical University (no.KLLY (A)-2019-043) and were performed according to the Guide for the Care and Use of Laboratory Animals (National Research Council (US) Committee for the Update of the Guide for the Care and Use of Laboratory Animals, 2011).

Perfusion protocol. Rats were anaesthetized with sodium pentobarbital (40 mg/kg) by intraperitoneal injection. The heart was quickly isolated and placed in K-H solution (1.19 mM KH_2PO_4, 11.1 mM glucose, 4.75 mM KCl, 1.19 mM $MgCl_2•6H_2O$, 2.50 mM $CaCl_2$ and 24.80 mM $NaHCO_3$, 118.00 mM NaCl, 4°C, pH 7.40). Then, the heart was rapidly connected to a Langendorff perfusion system. All hearts were perfused by a Langendorff apparatus with K-H solution for 20 min for equilibration. The rat hearts were randomly divided into four groups, including the Nor, I/R, DZ and 5-HD + DZ groups (n = 6/group). Hearts in the Nor group were continuously perfused with K-H solution with oxygen for 120 min. After 20 min of equilibration, hearts in the I/R w group ere perfused with St. Thomas solution (1.20 mM $CaCl_2$, 110.00 mM NaCl, 16.00 mM $MgCl_2$, 10.0 mM $NaHCO_3$, 16.00 mM KCl, 4°C) for ischemia for 40 min and then were perfused with K-H solution for 60 min. After ischemia, hearts in the DZ group were perfused with K-H solution containing diazoxide (50 μM) for 5 min before reperfusion and then with K-H solution for 55 min. Hearts in the 5-HD + DZ group were perfused with 5-hydroxydecanote (50 μM in K-H solution) for 5 min, perfused with diazoxide (50 μM) for 5 min, and then with K-H solution for 50 min. The protocols are outlined in Figure 1. At the end of reperfusion, the ventricular tissues were collected and stored at −80°C. At the end of equilibration (T1) and reperfusion (T2), the heart rate (HR), left ventricular developed pressure (LVDP), left ventricular end-diastolic pressure (LVEDP), and maximum left ventricular pressure (+dp/dt$_{max}$) were recorded by the Langendorff perfusion system.

Transmission electron microscopy (TEM). Myocardial tissue (1 mm³) at the end of reperfusion was fixed with 2.5% glutaraldehyde electron microscopic fixative, rinsed with PBS and then fixed with 1% osmic acid. The tissues were dehydrated with acetone and embedded using epoxy resin (35°C overnight, 45°C for 8 h, 60°C for 48 h). Myocardial sections were stained with uranyl acetate and lead citrate for 20 min. The myocardial ultrastructure was examined using an electron microscope (HITACHI-H7500, Hitachi, Japan), and mitochondrial damage was evaluated using the Flameng scoring method for each group (n = 6) (Flameng et al., 1980).

Metabonomics analysis. In total, 25 mg of myocardial tissue samples and 800 μl of methanol and acetonitrile were mixed for each group (n = 6). The mixture was sonicated for 10 min and centrifuged at 25,000 rpm for 15 min. The resulting supernatants were transferred to LC-MS vials and stored at −80°C. Quality control (QC) samples were prepared by mixing equal aliquots of the supernatants from all of the samples. LC-MS/MS analysis was performed using an UHPLC system (Waters 2D; Waters, United States) with a high-resolution mass spectrometer (Q Exactive; Thermo Fisher Scientific, United States). Mobile phase A was 0.1% formic acid in water for the positive ion mode and 10 mM ammonia formate in water for the negative ion mode, and mobile phase B was 10 mM ammonia formate in 95% methanol.

Raw MS data were filtered using the following criterion: less than 50% of all sample numbers in a group contained a metabolite (QC samples were also taken as a group). Missing values were replaced by
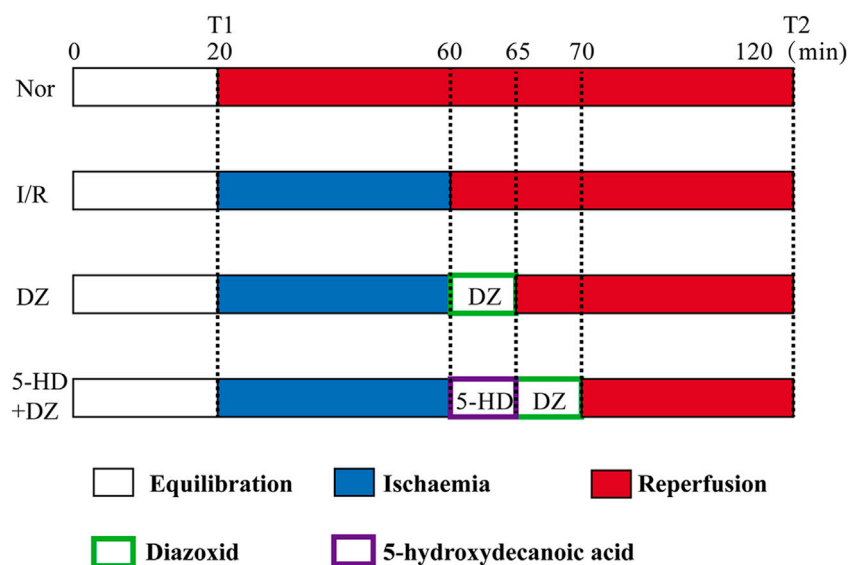
FIGURE 1
Perfusion protocol for isolated hearts.

half of the minimum value in the dataset by default. OSI-SMMS (Version 1.0, Dalian Chem Data Solution Information Technology Co. Ltd.) was used for the self-built database after XCMS (Version 3.2) data processing. The repeated metabolites from the positive and negative ion modes were merged. The variable importance in projection (VIP) score of the PLS-DA model was applied to rank the metabolites that best distinguished between comparisons. A t-test was also used for univariate analysis to screen differential metabolites. Metabolites with $p < 0.05$ and VIP ≥ 1 were considered differential metabolites between comparisons. Metabolites were mapped to KEGG metabolic pathways for pathway and enrichment analyses. $p < 0.05$ was considered statistically significant. Pathways meeting this condition were defined as significantly enriched pathways for differential metabolites.

Statistical analysis. Statistical analyses were performed using SPSS (Version 22.0, IBM Corp., Armonk, NY, and United States). Normally distributed data are presented as the mean ± SD. Groups were compared using Student's t test (normally distributed data). Two-way ANOVA followed by Sidak's multiple comparisons test was used to compare haemodynamic parameters at the same time point in different groups. Comparisons of the Flameng scores among different groups were conducted using the Kruskal-Wallis test followed by Dunn's *post hoc* test for multiple comparisons. To identify correlations between metabolite levels and the LVDP, stepwise multivariate linear regression was used, and Pearson's correlation analysis was applied using MetaboAnalyst 4.0.

Result

Diazoxide postconditioning improves cardiac function. There was no statistical significance in the comparison of HR, LVDP, +dp/dt$_{max}$ and LVEDP among the four groups at T1. The HR, LVDP and +dp/dt$_{max}$ of the Nor group and the DZ group at T2 were significantly higher than those of the I/R and 5-HD + DZ groups (Figures 2A–C), whereas the LVEDP of the Nor group and the DZ group at T2 was lower than that of the I/R and 5-HD + DZ groups (Figure 2D). These findings suggested that diazoxide postconditioning improved I/R-induced haemodynamic dysfunction, which was abolished by treatment with its blocker 5-HD.

Myocardial ultrastructure and the Flameng score. The myofilaments in the I/R and 5-HD + DZ groups were ruptured, dissolved and disordered. Moreover, the mitochondria were dissolved and destroyed (Figures 3B, D). In the DZ group, myocardial morphology was basically normal, and fewer myofilaments were dissolved. Most mitochondria in the DZ group were intact, but a few of them were slightly swollen (Figures 3A, C). The Flameng score in the DZ group was lower than that in the I/R group ($p < 0.001$) (Figure 3E). However, the Flameng score in the 5-HD + DZ group was significantly higher than that in the DZ group ($p < 0.001$) (Figure 3E).

Multivariate statistical analysis. A partial least squares discriminant (PLS-DA) model was built using a dataset including the four groups of samples. R2Y and Q2 represent the interpretation rate of the Y matrix and the predicted variation, respectively, with parameters as follows: R2Y = 0.90, Q2 = 0.26 (Nor group *vs.* I/R group); R2Y = 0.98, Q2 = 0.84 (DZ group *vs.* I/R group); and R2Y = 0.95, Q2 = 0.63 (DZ group *vs.* 5-HD + DZ group). The score plots revealed that each class was well separated, suggesting that the PLS-DA model successfully discriminated samples according to their underlying metabolic profiles (Figures 4A–C).

Identification of potential regulated metabolites. The PLS-DA model was used to screen differential metabolites. Metabolites with $p < 0.05$ and VIP ≥ 1 were considered differential metabolites between comparisons. The levels of ten metabolites were significantly decreased after myocardial ischemia/reperfusion injury, while the levels of eight metabolites increased (Table 1).
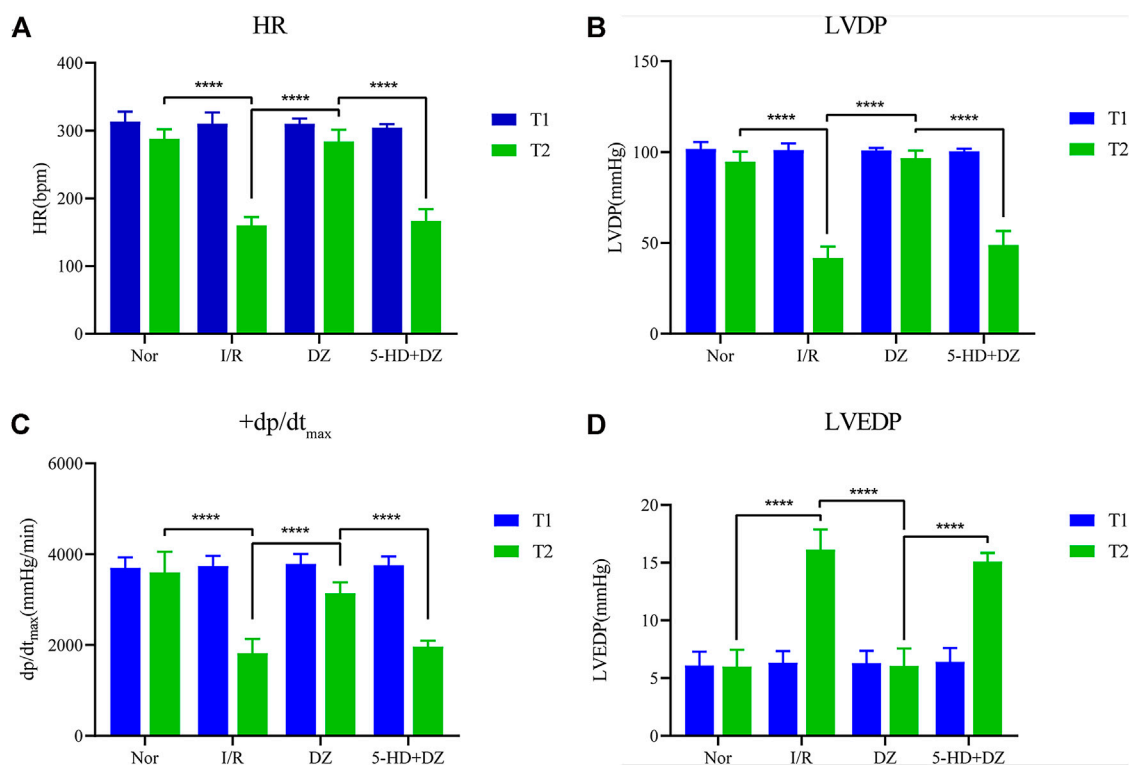
FIGURE 2
Haemodynamic parameters. Diazoxide postconditioning improves HR **(A)**, LVDP **(B)**, dp/dtmax **(C)** and LVEDP **(D)** after MIRI, whereas 5-HD eliminates the effect (comparisons at different time points in the same group and comparisons at the same time point in different groups were conducted using two-way ANOVA followed by Sidak's *post hoc* test). ***$p < 0.001$. HR, heart rate; dp/dtmax, maximum rate of the rise in intraventricular pressure; LVDP, left ventricular developed pressure; LVEDP, left ventricular end-diastolic pressure.

The levels of eight metabolites were significantly decreased after diazoxide postconditioning, while ten metabolites increased (Table 2). The levels of five metabolites were significantly decreased after 5-hydroxydecanoic acid and diazoxide postconditioning, while six metabolites increased (Table 3). The significantly changed metabolites between the Nor and I/R groups are presented as heatmaps in the Supplementary Material (Figure 5A). The significantly changed metabolites between the DZ and I/R groups are presented as heatmaps in the Supplementary Material (Figure 5B). The significantly changed metabolites between the DZ and 5-HD + DZ groups are presented as heatmaps in the Supplementary Material (Figure 5C). Our results showed that the levels of nicotinic acid, citric acid, L-threonine and L-lysine in the Nor and DZ groups were higher than those in the I/R group. The levels of nicotinic acid in the DZ group were higher than those in the I/R and 5-HD + DZ groups. The levels of L-glutamic acid in the DZ group were lower than those in the I/R and 5-HD + DZ groups.
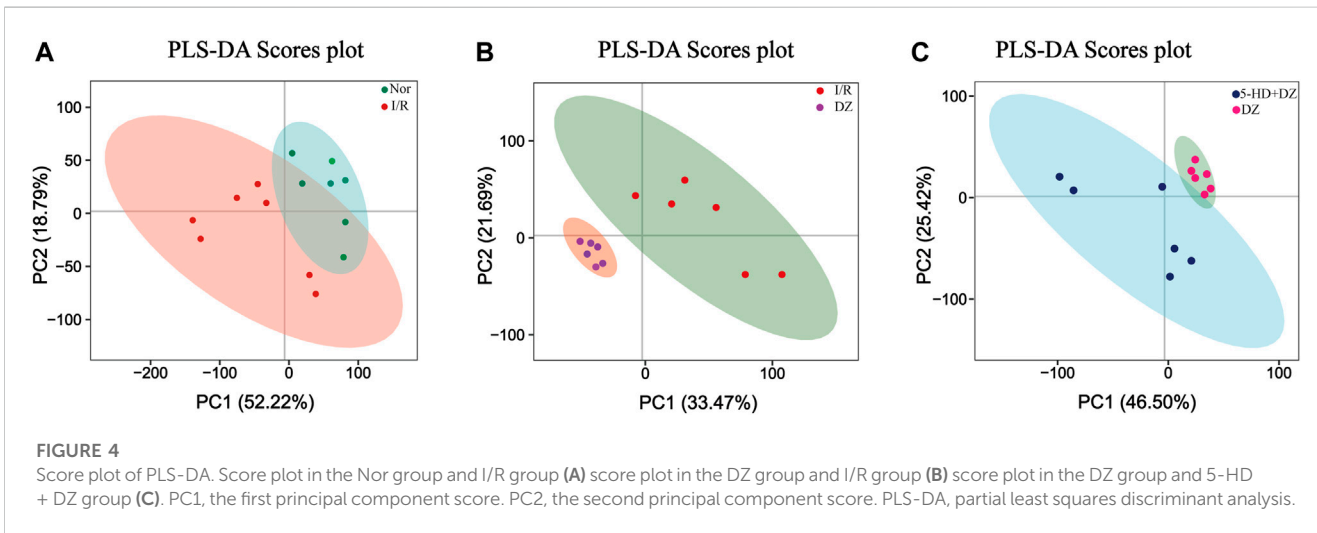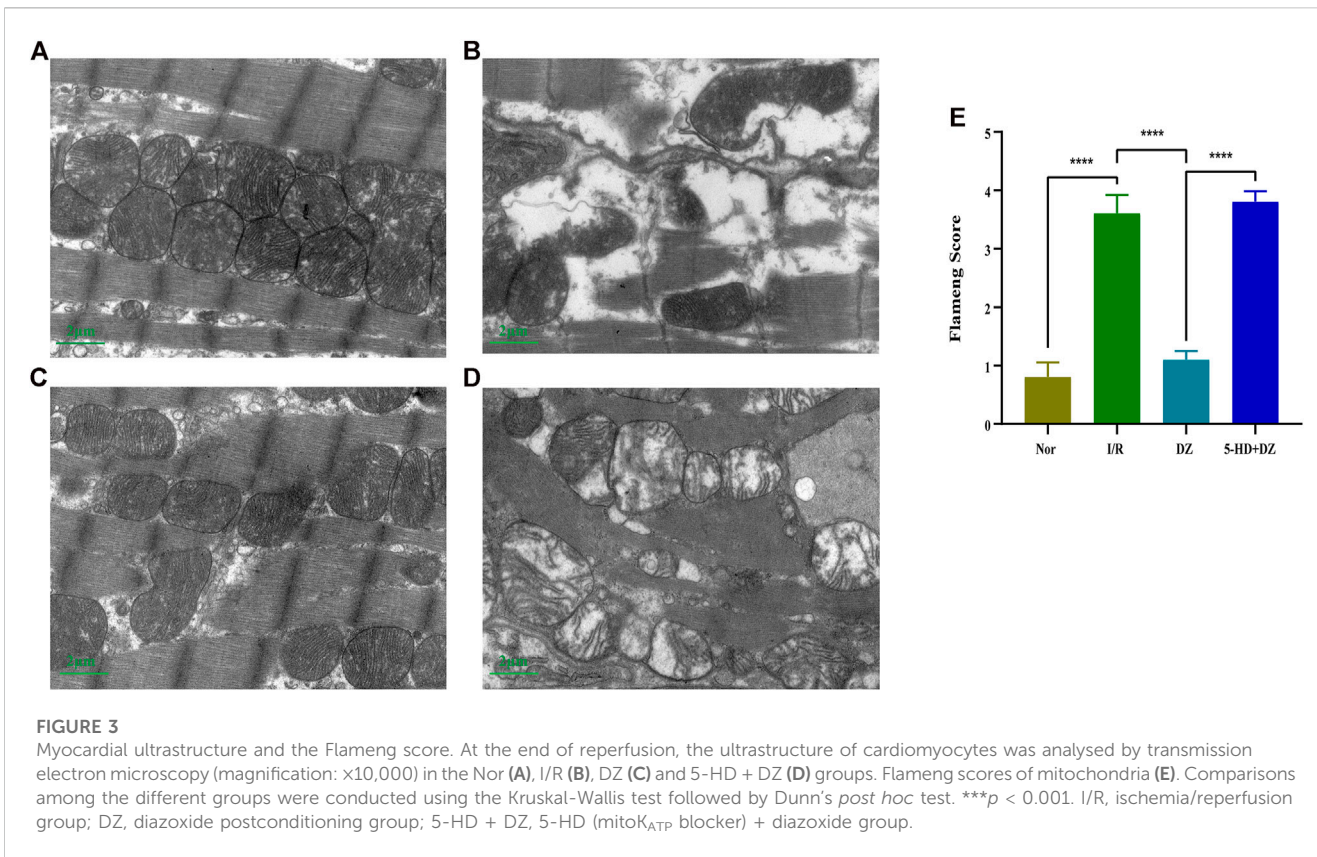
Biological pathway analysis. Pathway analysis was applied to investigate the biological functions of the altered metabolites. Multiple metabolic pathways were impacted after MIRI and diazoxide postconditioning in both the Nor group and the I/R group (Figure 6A), both the DZ group and the I/R group (Figure 6B), and both the DZ group and the 5-HD + DZ group (Figure 6C), mainly including the tricarboxylic acid cycle, nicotinate

and nicotinamide metabolism, glutamate metabolism, glutathione metabolism, and aminoacyl-tRNA biosynthesis.

Changes in five metabolites are relevant to diazoxide postconditioning. Correlation analysis was used to determine the metabolites related to diazoxide postconditioning in MIRI. Finally, we identified five metabolites that may be relevant to diazoxide postconditioning: L-glutamic acid (LVDP: $p = 0.0036$), L-threonine (LVDP: $p = 0.0400$), citric acid (LVDP: $p = 0.0400$), succinate (LVDP: $p = 0.0036$), and nicotinic acid (LVDP: $p = 0.0317$) (Figure 5D).

Discussion

In this study, diazoxide postconditioning was found to significantly reduce myocardial ischemia-reperfusion injury, which is consistent with our previous results (Cao et al., 2015; Pan et al., 2020; Chen et al., 2021). The present study indicated that MIRI disturbed multiple metabolic changes, including decreased levels of citrate, nicotinate, L-threonine, and L-lysine. However, diazoxide postconditioning increased the levels of these metabolites. In addition, MIRI also increased the levels of succinate and L-glutamic acid. However, the levels of these metabolites were decreased after diazoxide postconditioning. Our results suggest that the TCA cycle and amino acid metabolism might be

FIGURE 3
Myocardial ultrastructure and the Flameng score. At the end of reperfusion, the ultrastructure of cardiomyocytes was analysed by transmission electron microscopy (magnification: ×10,000) in the Nor **(A)**, I/R **(B)**, DZ **(C)** and 5-HD + DZ **(D)** groups. Flameng scores of mitochondria **(E)**. Comparisons among the different groups were conducted using the Kruskal-Wallis test followed by Dunn's *post hoc* test. ***$p < 0.001$. I/R, ischemia/reperfusion group; DZ, diazoxide postconditioning group; 5-HD + DZ, 5-HD (mitoK$_{ATP}$ blocker) + diazoxide group.

FIGURE 4
Score plot of PLS-DA. Score plot in the Nor group and I/R group **(A)** score plot in the DZ group and I/R group **(B)** score plot in the DZ group and 5-HD + DZ group **(C)**. PC1, the first principal component score. PC2, the second principal component score. PLS-DA, partial least squares discriminant analysis.

relevant to MIRI and the myocardial protective mechanism of diazoxide postconditioning.

The TCA cycle, also known as the citric acid cycle (CAC) or Krebs cycle, is a significant pathway for various nutrients, including glucose, fatty acids, and amnio acids, and eventually produces ATP through oxidative phosphorylation (LaNoue et al., 1970). Citric acid is an important intermediate in the TCA cycle and is produced from oxaloacetate and acetyl-CoA.

In the TCA cycle, citric acid is converted into α-ketoglutarate (α-KG) via isocitrate by isocitrate dehydrogenase (IDH) (Akram, 2014). Citric acid plays a significant role in inflammatory response-related pathways and is connected with several important proinflammatory mediators, including NO, ROS and prostaglandin E$_2$ (PGE$_2$) (Williams and O'Neill, 2018). A previous study found that the level of citric acid was decreased after MIRI (Mu et al., 2017), which was consistent with our findings.

TABLE 1 Significantly differential metabolites in heart tissues between Nor and I/R group.

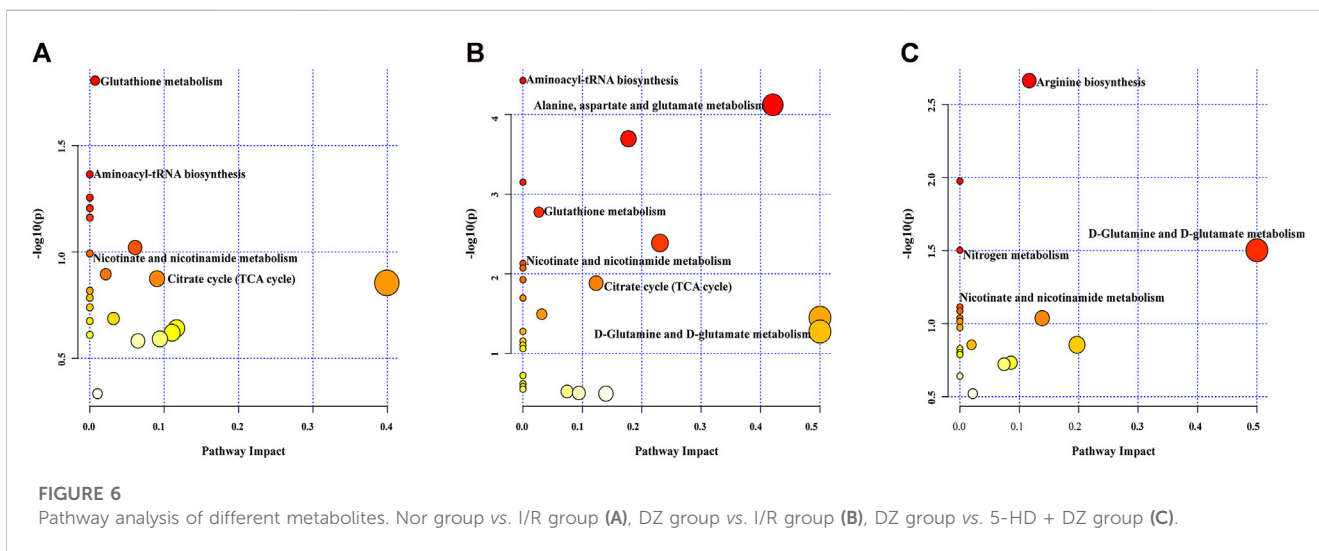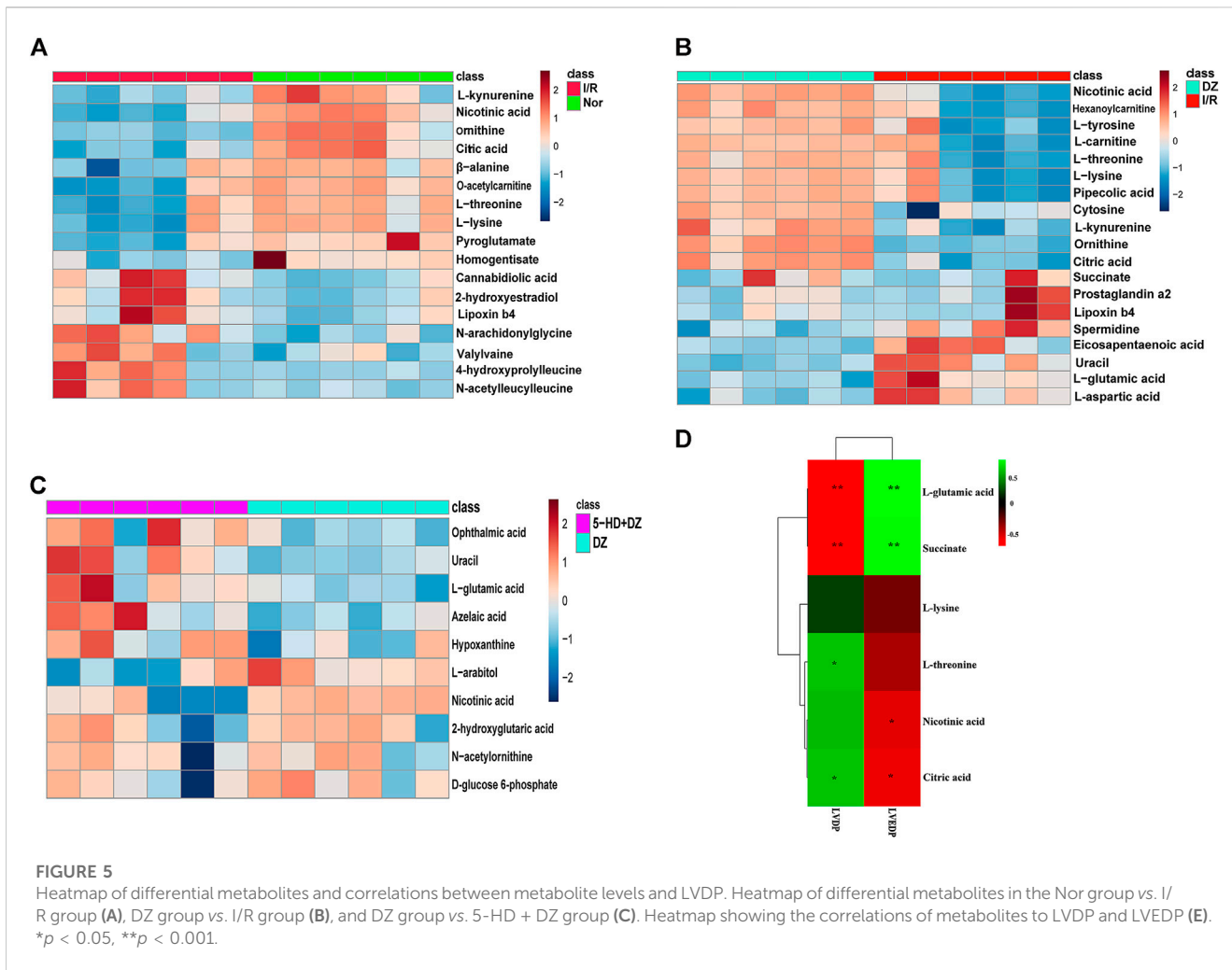| Metabolites	Formula	VIP	p-value	FC
4-hydroxyprolylleucine	$C_{11} H_{20} N_2 O_4$	1.5048	0.0384	58.6213
N-acetylleucylleucine	$C_{14} H_{26} N_2 O_4$	1.423	0.0424	47.5131
2-hydroxyestradiol	$C_{18} H_{24} O_3$	1.422	0.0443	29.5835
N-arachidonylglycine	$C_{22} H_{35} N O_3$	1.2318	0.0046	3.5885
Cannabidiolic acid	$C_{22} H_{30} O_4$	1.2007	0.0119	6.0837
Lipoxin b4	$C_{20} H_{32} O_5$	1.1962	0.0404	9.6321
Prostaglandin g2	$C_{20} H_{32} O_6$	1.1885	0.0406	17.930
Valylvaline	$C_{10} H_{20} N_2 O_3$	1.0222	0.0384	3.3415
Nicotinic acid	$C_6 H_5 N O_2$	2.1749	0.0005	−0.0449
O-acetylcarnitine	$C_9 H_{17} N O_4$	2.0184	0.0150	−0.1905
Ornithine	$C_5 H_{12} N_2 O_2$	1.9882	0.0021	−0.0992
Pyroglutamate	$C_5 H_7 N O_3$	1.7696	0.0091	−0.1066
Citric acid	$C_6 H_8 O_7$	1.6698	0.0008	−0.1503
Homogentisate	$C_8 H_8 O_4$	1.544	0.0247	−0.1291
L-kynurenine	$C_{10} H_{12} N_2 O_3$	1.4219	0.0116	−0.1606
L-threonine	$C_4 H_9 N O_3$	1.1585	0.0237	−0.4020
L-lysine	$C_6 H_{14} N_2 O_2$	1.112	0.0203	−0.4253
B-alanine	$C_3 H_7 N O_2$	1.1018	0.0448	−0.3569

FC, Fold change; VIP, Variable importance.

TABLE 2 Significantly differential metabolites in heart tissues between DZ vs. I/R group.

Metabolites	Formula	VIP	p-value	FC
Uracil	$C_4 H_4 N_2 O_2$	1.7776	0.0034	0.0809
Eicosapentaenoic acid	$C_{20} H_{30} O_2$	1.4318	0.0163	0.2139
L-aspartic acid	$C_4 H_7 N O_4$	1.3743	0.0053	0.1461
Prostaglandin a2	$C_{20} H_{30} O_4$	1.2555	0.048	0.1325
Lipoxin b4	$C_{20} H_{32} O_5$	1.2416	0.0485	0.0995
L-glutamic acid	$C_5 H_9 N O_4$	1.2415	0.0117	0.2673
Succinate	$C_4 H_6 O_4$	1.224	0.0139	0.2668
Spermidine	$C_7 H_{19} N_3$	1.1164	0.0044	0.4652
Nicotinic acid	$C_6 H_5 N O_2$	2.3879	0.0011	−14.7018
Hexanoylcarnitine	$C_{13} H_{25} N O_4$	2.1384	0.0095	−4.9302
Ornithine	$C_5 H_{12} N_2 O_2$	2.0173	0.0000	−8.6706
L-carnitine	$C_7 H_{15} N O_3$	2.0143	0.0465	−1.8073
Citric acid	$C_6 H_8 O_7$	1.8272	0.0001	−5.7788
L-threonine	$C_4 H_9 N O_3$	1.3456	0.0387	−2.0369
L-lysine	$C_6 H_{14} N_2 O_2$	1.3272	0.0309	−2.0230
Pipecolic acid	$C_6 H_{11} N O_2$	1.3338	0.0307	−2.0331
Cytosine	$C_4 H_5 N_3 O$	1.3068	0.0199	−2.9574
L-kynurenine	$C_{10} H_{12} N_2 O_3$	1.2496	0.0004	−3.3334
L-tyrosine	$C_9 H_{11} N O_3$	1.1905	0.0397	−1.8692

FC, Fold change; VIP, Variable importance.

In the present research, the citric acid content was increased after diazoxide postconditioning. In the TCA cycle, succinate is produced from α-KG via succinyl CoA synthase and converted into fumarate via succinate dehydrogenase (SDH) (Huang and Millar, 2013). During ischemia, the accumulation of succinate is caused by reversal of SDH, which might convert fumarate to succinate. Following reperfusion, abundant succinate is rapidly oxidized and drives reverse electron transport (RET) to generate massive reactive oxygen species (ROS) at mitochondrial complex I (Chouchani et al., 2014; Kula-Alwar et al., 2019). Early studies revealed that extensive ROS induce serious acute damage and variations in pathology (Granger and Kvietys, 2015; Bystrom et al., 2017; Cadenas, 2018). ROS trigger mitochondrial permeability transition pore (mPTP) opening in conjunction with alterations in Ca^{2+} levels and physiological pH, aggravating MIRI (Cadenas, 2018; Bugger and Pfeil, 2020). Evidence indicates that inhibiting SDH reduces the content of succinate and ROS production, thus protecting cardiac function from MIRI (Valls-Lacalle et al., 2018; Xu et al., 2018). Our previous result showed that diazoxide postconditioning can decrease ROS level (Chen et al., 2021). This study showed that the level of succinate decreased after diazoxide postconditioning, which may be involved in inhibiting SDH (Anastacio et al., 2013). The cardioprotective effect of diazoxide postconditioning may be associated with regulating CAC intermediates and maintaining the normal function of the CAC.

TABLE 3 Significantly differential metabolites in heart tissues between DZ vs. 5-HD + DZ group.

Metabolites	Formula	VIP	P	FC
Uracil	$C_4 H_4 N_2 O_2$	1.6671	0.0221	7.4379
Sebacic acid	$C_{10} H_{18} O_4$	1.5291	0.0127	2.9046
Ophthalmic acid	$C_{11} H_{19} N_3 O_6$	1.2602	0.039	2.2042
Azelaic acid	$C_9 H_{16} O_4$	1.2346	0.0283	1.9060
L-glutamic acid	$C_5 H_9 N O_4$	1.183	0.0313	2.7131
Hypoxanthine	$C_5 H_4 N_4 O$	1.0309	0.0462	1.5543
Nicotinic acid	$C_6 H_5 N O_2$	3.0196	0.0316	−0.2919
2-hydroxyglutaric acid	$C_5 H_8 O_5$	1.8662	0.0142	−0.3227
N-acetylornithine	$C_7 H_{14} N_2 O_3$	1.154	0.0389	−0.5583
L-arabitol	$C_5 H_{12} O_5$	1.1321	0.0378	−0.5208
D-glucose 6-phosphate	$C_6 H_{13} O_9 P$	1.0887	0.0313	−0.5526

FC, Fold change; VIP, Variable importanc.

Nicotinic acid (NA) and nicotinamide, which are known as vitamin B3, are precursors of nicotinamide adenine dinucleotide (NAD^+) and nicotinamide adenine phosphate (NADP) (Cantó et al.,

FIGURE 5

Heatmap of differential metabolites and correlations between metabolite levels and LVDP. Heatmap of differential metabolites in the Nor group *vs.* I/R group **(A)**, DZ group *vs.* I/R group **(B)**, and DZ group *vs.* 5-HD + DZ group **(C)**. Heatmap showing the correlations of metabolites to LVDP and LVEDP **(E)**. *p < 0.05, **p < 0.001.

FIGURE 6

Pathway analysis of different metabolites. Nor group *vs.* I/R group **(A)**, DZ group *vs.* I/R group **(B)**, DZ group *vs.* 5-HD + DZ group **(C)**.

2015). NAD⁺ plays a significant role in diverse metabolic pathways, including the CAC and oxidative phosphorylation (OXPHOS), glycolysis, fermentation, cell signalling and inflammatory pathways (Yang and Sauve, 2016). NAD⁺ is converted into NADH by accepting hydride groups in normal oxidation. Then, NADH is oxidized to produce ATP in mitochondria through

OXPHOS, which is responsible for 95% of the ATP production in the heart (Matasic et al., 2018). The function of OXPHOS was impaired by MIRI due to a series of enzymes, such as NADH oxidase or mitochondrial ROS release. Many studies have confirmed that increasing NAD+ during MIRI could mitigate oxidative stress and alleviate myocardial injury (Trueblood et al., 2000; Yamamoto et al., 2014; Tai et al., 2015). In the present study, the NA content significantly decreased after I/R, while the NA content increased after diazoxide postconditioning, indicating that diazoxide may exert protective effects by regulating NA and NAD+ concentrations.

Glutamate is an important excitatory neurotransmitter in the central nervous system and is associated with cerebral I/R injury (Kim et al., 2017; Leung et al., 2020; Song et al., 2020). In addition, glutamate receptors and transporters exist in peripheral tissues, such as the heart, lung, kidney and liver (Du et al., 2016). Currently, the effect of glutamate on the heart is still controversial. Studies have claimed that exogenous glutamate supplementation may alleviate injury caused by myocardial ischemia (Kristiansen et al., 2008; Sufit et al., 2012 no date). However, several studies hold the contrary opinion. One study demonstrated that the concentration of glutamate was elevated after 15 min of reperfusion in a rat cardiac transplantation model (Venturini et al., 2009). Additionally, Sun et al. (2014) claimed that the serum glutamate concentration increased after I/R and mediated ventricular arrhythmias by inducing Ca^{2+} accumulation, which may be mediated by initiating voltage-dependent Ca^{2+} channels and NMDA receptor channels (Piccirillo et al., 2020). Yokoyama et al. (2019) showed that mitoKATP opening can suppress glutamate release to reduce neuronal injury induced by I/R in the brain. Consistently, our results demonstrate that the level of L-glutamic acid in the DZ group was lower than that in the I/R and 5-HD + DZ groups. The mechanism of glutamate release in MIRI is quite complicated and should be determined in future studies.

L-Threonine is an essential amino acid in the human body and plays a significant role in lipid metabolism (Chen et al., 2022). Under anaerobic conditions, L-threonine is converted to keto acid, which produces ATP via substrate-level phosphorylation to provide a source of energy to the cells (Simanshu et al., 2007). Research has reported that L-threonine may participate in the innate immune response by activating the NF-κB signalling pathway and suppressing sirtuin-1 (SIRT1) (Wu et al., 2018). Recently, studies have proven that both the NF-κB signalling pathway and SIRT1 are associated with MIRI (Xu et al., 2021; Aghamohammad et al., 2022; Xiao et al., 2022). The cardiovascular protective effect of the NF-κB signalling pathway is related to regulating the inflammatory response (Dong et al., 2022). SIRT1, an NAD+-dependent deacetylase, plays a significant role in antioxidative stress activity (Zhang et al., 2017). Lysine is an indispensable amino acid. Zhang et al. (2019) reported that L-lysine supplementation may ameliorate proinflammatory changes by reducing lipid peroxidation and proinflammatory mediators, including tumour necrosis factor α (TNFα), interleukin-8 and macrophage inhibitory factor, to protect against acute lung injury. Furthermore, lysine is one of the amino acid groups most susceptible to modification (Moreno-Yruela et al., 2022). In recent years, lysine methylation, lysine succinylation, and lysine acetylation have been closely associated with cardiovascular disease and have

provided a new theoretical basis for the treatment of heart disease (Boylston et al., 2015; Yi et al., 2017; Herr et al., 2020). Although the effects of L-threonine and L-lysine on MIRI have not been reported, our study found that the level of L-threonine after MIRI was decreased, which can be alleviated by diazoxide postconditioning, suggesting that these metabolite changes might be relevant to MIRI and the myocardial protective mechanism of diazoxide postconditioning.

Study limitations

The present study has several limitations. First, we should add 5-HD group to make our results more rigor and we will consider this in future study. Seconed, the solated hearts of langendorff may not be an appropriate model for studying myocardial ischemia/reperfusion injury. It will be interesting to explore the effects of diazoxide postconditioning on ischemia/reperfusion injury using a classic ischemia/reperfusion method, and further compared the results between different ischemia/reperfusion methods. Third, we did not perform *in vivo* experiments to confirm the metabolic changes and protective effects of diazoxide postconditioning in MIRI. Four, we did not validate the function of these identified metabolites or the associated pathways in MIRI.

Conclusion

In summary, the present study indicated that diazoxide postconditioning may improve MIRI via certain metabolic changes, including changes in the levels of citrate, nicotinic acid, L-glutamic acid, L-threonine and L-lysine. This study provides resource data for future studies on metabolism relevant to diazoxide postconditioning and MIRI.

Data availability statement

The original contributions presented in the study are included in the article/Supplementary Materials, further inquiries can be directed to the corresponding author.

Ethics statement

The animal study was reviewed and approved by the Animal Care and Use Committee of Zunyi Medical University. Written informed consent was obtained from the owners for the participation of their animals in this study.

Author contributions

YW and DZ designed the study. CX, SY, and BJ performed the study. CX analysed the data, CX wrote the manuscript. JL and QR wrote sections of the manuscript. All authors contributed to the article and approved the submitted version.

Funding

Conflict of interest

The authors declare that the research was conducted in the absence of any commercial or financial relationships that could be construed as a potential conflict of interest.

Publisher's note

Supplementary material

The Supplementary Material for this article can be found online at: https://www.frontiersin.org/articles/10.3389/fmolb.2023.1196894/full#supplementary-material

References

Aghamohammad, S., Sepehr, A., Miri, S. T., Najafi, S., Rohani, M., and Pourshafiea, M. R. (2022). The effects of the probiotic cocktail on modulation of the NF-kB and JAK/STAT signaling pathways involved in the inflammatory response in bowel disease model. *BMC Immunol.* 23 (1), 8. doi:10.1186/s12865-022-00484-6

Akram, M. (2014). Citric acid cycle and role of its intermediates in metabolism. *Cell Biochem. Biophysics* 68 (3), 475–478. doi:10.1007/s12013-013-9750-1

Anastacio, M. M., Kanter, E. M., Makepeace, C., Keith, A. D., Zhang, H., Schuessler, R. B., et al. (2013). Cardioprotective mechanism of diazoxide involves the inhibition of succinate dehydrogenase. *Ann. Thorac. Surg.* 95 (6), 2042–2050. doi:10.1016/j.athoracsur.2013.03.035

Boylston, J. A., Sun, J., Chen, Y., Gucek, M., Sack, M. N., and Murphy, E. (2015). Characterization of the cardiac succinylome and its role in ischemia-reperfusion injury. *J. Mol. Cell. Cardiol.* 88, 73–81. doi:10.1016/j.yjmcc.2015.09.005

Bugger, H., and Pfeil, K. (2020). Mitochondrial ROS in myocardial ischemia reperfusion and remodeling. *Biochimica Biophysica Acta (BBA) - Mol. Basis Dis.* 1866 (7), 165768. doi:10.1016/j.bbadis.2020.165768

Bystrom, P., Foley, N., Toledo-Pereyra, L., and Quesnelle, K. (2017). Ischemic preconditioning modulates ROS to confer protection in liver ischemia and reperfusion. *EXCLI J.* 16, 483–496. doi:10.17179/excli2017-166

Cadenas, S. (2018). ROS and redox signaling in myocardial ischemia-reperfusion injury and cardioprotection. *Free Radic. Biol. Med.* 117, 76–89. doi:10.1016/j.freeradbiomed.2018.01.024

Cantó, C., Menzies, K. J., and Auwerx, J. (2015). NAD(+) metabolism and the control of energy homeostasis: A balancing act between mitochondria and the nucleus. *Cell Metab.* 22 (1), 31–53. doi:10.1016/j.cmet.2015.05.023

Cao, S., Yun, L., Wenting, S., Li, Z., Lin, Z., Xinkui, L., et al. (2015) Genome-wide expression profiling of anoxia/reoxygenation in rat cardiomyocytes uncovers the role of mito K ATP in energy homeostasis', *Oxidative Med. Cell. Longev.* 1–14. doi:10.1155/2015/756576

Chen, J., Qian, D., Wang, Z., Sun, Y., Sun, B., Zhou, X., et al. (2022). Threonine supplementation prevents the development of fat deposition in mice fed a high-fat diet. *Food & Funct.* 13 (14), 7772–7780. doi:10.1039/d2fo01201d

Chen, X.-Y., Wang, J. Q., Cheng, S. J., Wang, Y., Deng, M. Y., Yu, T., et al. (2021). Diazoxide post-conditioning activates the HIF-1/HRE pathway to induce myocardial protection in hypoxic/reoxygenated cardiomyocytes. *Front. Cardiovasc. Med.* 8. doi:10.3389/fcvm.2021.711465

Chouchani, E. T., Pell, V. R., Gaude, E., Aksentijević, D., Sundier, S. Y., Robb, E. L., et al. (2014). Ischaemic accumulation of succinate controls reperfusion injury through mitochondrial ROS. *Nature* 515 (7527), 431–435. doi:10.1038/nature13909

Dong, P., Liu, K., and Han, H. (2022). The role of NF-κB in myocardial ischemia/reperfusion injury. *Curr. protein & peptide Sci.* 23 (8), 535–547. doi:10.2174/1389203723666220817085941

Du, J., Li, X.-H., and Li, Y.-J. (2016). Glutamate in peripheral organs: Biology and pharmacology. *Eur. J. Pharmacol.* 784, 42–48. doi:10.1016/j.ejphar.2016.05.009

Flameng, W., Borgers, M., Daenen, W., and Stalpaert, G. (1980). Ultrastructural and cytochemical correlates of myocardial protection by cardiac hypothermia in man. *J. Thorac. Cardiovasc. Surg.* 79 (3), 413–424. doi:10.1016/s0022-5223(19)37950-4

Granger, D. N., and Kvietys, P. R. (2015). Reperfusion injury and reactive oxygen species: The evolution of a concept. *Redox Biol.* 6, 524–551. doi:10.1016/j.redox.2015.08.020

Herr, D. J., Singh, T., Dhammu, T., and Menick, D. R. (2020). Regulation of metabolism by mitochondrial enzyme acetylation in cardiac ischemia-reperfusion injury. *Biochimica Biophysica Acta (BBA) - Mol. Basis Dis.* 1866 (6), 165728. doi:10.1016/j.bbadis.2020.165728

Huang, S., and Millar, A. H. (2013). Succinate dehydrogenase: The complex roles of a simple enzyme. *Curr. Opin. plant Biol.* 16 (3), 344–349. doi:10.1016/j.pbi.2013.02.007

Jin, L., Zhou, W., Chen, W., Wang, H., Zhang, Y., and Yu, T. (2020). Mechanism of the hypoxia inducible factor 1/hypoxic response element pathway in rat myocardial ischemia/diazoxide post-conditioning. *Mol. Med. Rep.* 21 (3), 1527–1536. doi:10.3892/mmr.2020.10966

Kim, A. Y., Jeong, K. H., Lee, J. H., Kang, Y., Lee, S. H., and Baik, E. J. (2017). Glutamate dehydrogenase as a neuroprotective target against brain ischemia and reperfusion. *Neuroscience* 340, 487–500. doi:10.1016/j.neuroscience.2016.11.007

Kolwicz, S. C., Purohit, S., and Tian, R. (2013). Cardiac metabolism and its interactions with contraction, growth, and survival of cardiomyocytes. *Circulation Res.* 113 (5), 603–616. doi:10.1161/CIRCRESAHA.113.302095

Kristiansen, S. B., Løfgren, B., Støttrup, N. B., Kimose, H. H., Nielsen-Kudsk, J. E., Bøtker, H. E., et al. (2008). Cardioprotection by L-glutamate during postischaemic reperfusion: Reduced infarct size and enhanced glycogen resynthesis in A rat insulin-free heart model. *Clin. Exp. Pharmacol. Physiology* 35 (8), 884–888. doi:10.1111/j.1440-1681.2008.04914.x

Kula-Alwar, D., Prag, H. A., and Krieg, T. (2019). Targeting succinate metabolism in ischemia/reperfusion injury. *Circulation* 140 (24), 1968–1970. doi:10.1161/CIRCULATIONAHA.119.042791

LaNoue, K., Nicklas, W. J., and Williamson, J. R. (1970). Control of citric acid cycle activity in rat heart mitochondria. *J. Biol. Chem.* 245 (1), 102–111. doi:10.1016/s0021-9258(18)63427-1

Leung, S. W., Lai, J. H., Wu, J. C. C., Tsai, Y. R., Chen, Y. H., Kang, S. J., et al. (2020). Neuroprotective effects of emodin against ischemia/reperfusion injury through activating ERK-1/2 signaling pathway. *Int. J. Mol. Sci.* 21 (8), 2899. doi:10.3390/ijms21082899

Matasic, D. S., Brenner, C., and London, B. (2018). Emerging potential benefits of modulating NAD $^+$ metabolism in cardiovascular disease. *Am. J. Physiology-Heart Circulatory Physiology* 314 (4), H839. doi:10.1152/ajpheart.00409.2017

Mironova, G. D., Rozova, E. V., Belosludtseva, N. V., and Man'kovskaya, I. N. (2019). Dynamic restructuring of the myocardial mitochondria in response to uridine modulation of the activity of mitochondrial ATP-dependent potassium channel under conditions of acute hypoxic hypoxia. *Bull. Exp. Biol. Med.* 166 (6), 806–810. doi:10.1007/s10517-019-04445-9

Moreno-Yruela, C., Bæk, M., Monda, F., and Olsen, C. A. (2022). Chiral posttranslational modification to lysine ε-amino groups. *Accounts Chem. Res.* 55 (10), 1456–1466. doi:10.1021/acs.accounts.2c00115

Mu, F., Duan, J., Bian, H., Zhai, X., Shang, P., Lin, R., et al. (2017). Metabonomic strategy for the evaluation of Chinese medicine *Salvia miltiorrhiza* and *Dalbergia odorifera* interfering with myocardial ischemia/reperfusion injury in rats. *Rejuvenation Res.* 20 (4), 263–277. doi:10.1089/rej.2016.1884

National Research Council (Us) *Committee for the update of the Guide for theCare and use of laboratory animals (2011)* Guide for the Care and Use of laboratory animals. Washington (DC): National Academies Press US. (The National Academies Collection: Reports funded by National Institutes of Health). Available at: http://www.ncbi.nlm.nih.gov/books/NBK54050/ (Accessed: November 27, 2022).

Onukwufor, J. O., Stevens, D., and Kamunde, C. (2016). Bioenergetic and volume regulatory effects of mitoKATP channel modulators protect against hypoxia-reoxygenation induced mitochondrial dysfunction. *J. Exp. Biol.* 219, 2743–2751. doi:10.1242/jeb.140186

Pan, Y., Wang, Y., Shi, W., Liu, Y., Cao, S., and Yu, T. (2020). Mitochondrial proteomics alterations in rat hearts following ischemia/reperfusion and diazoxide post-conditioning. *Mol. Med. Rep.* 23 (2), 161. doi:10.3892/mmr.2020.11800

Piccirillo, S., Magi, S., Castaldo, P., Preziuso, A., Lariccia, V., and Amoroso, S. (2020). NCX and EAAT transporters in ischemia: At the crossroad between glutamate metabolism and cell survival. *Cell Calcium* 86, 102160. doi:10.1016/j.ceca.2020.102160

Russo, I., Penna, C., Musso, T., Popara, J., Alloatti, G., Cavalot, F., et al. (2017). Platelets, diabetes and myocardial ischemia/reperfusion injury. *Cardiovasc. Diabetol.* 16 (1), 71. doi:10.1186/s12933-017-0550-6

Simanshu, D. K., Chittori, S., Savithri, H. S., and Murthy, M. R. N. (2007). Structure and function of enzymes involved in the anaerobic degradation of L-threonine to propionate. *J. Biosci.* 32 (6), 1195–1206. doi:10.1007/s12038-007-0121-1

Song, X., Gong, Z., Liu, K., Kou, J., Liu, B., and Liu, K. (2020). Baicalin combats glutamate excitotoxicity via protecting glutamine synthetase from ROS-induced 20S proteasomal degradation. *Redox Biol.* 34, 101559. doi:10.1016/j.redox.2020.101559

Sufit, A., Weitzel, L. B., Christine, H., Queensland, K., Dauber, I., Rooyackers, O., et al. (2012). Pharmacologically dosed oral glutamine reduces myocardial injury in patients undergoing cardiac surgery: A randomized pilot feasibility trial. *J. Parenter. Enter. Nutr.* 6, 556. doi:10.1177/0148607112448823

Sun, X., Zhong, J., Wang, D., Xu, J., Su, H., An, C., et al. (2014). Increasing glutamate promotes ischemia-reperfusion-induced ventricular arrhythmias in rats *in vivo*. *Pharmacology* 93 (1–2), 4–9. doi:10.1159/000356311

Tai, S. T., Yang, Y. C., and Wang, J. J. (2015). Niacin ameliorates kidney warm ischemia and reperfusion injury–induced ventricular dysfunction and oxidative stress and disturbance in mitochondrial metabolism in rats. *Transplant. Proc.* 47 (4), 1079–1082. doi:10.1016/j.transproceed.2014.11.057

Trueblood, N. A., Ramasamy, R., Wang, L. F., and Schaefer, S. (2000). Niacin protects the isolated heart from ischemia-reperfusion injury. *Am. J. Physiology-Heart Circulatory Physiology* 279 (2), H764–H771. doi:10.1152/ajpheart.2000.279.2.H764

Valls-Lacalle, L., Barba, I., Miró-Casas, E., Ruiz-Meana, M., Rodríguez-Sinovas, A., and García-Dorado, D. (2018). Selective inhibition of succinate dehydrogenase in reperfused myocardium with intracoronary malonate reduces infarct size. *Sci. Rep.* 8 (1), 2442. doi:10.1038/s41598-018-20866-4

Venturini, A., Ascione, R., Lin, H., Polesel, E., Angelini, G. D., and Suleiman, M. S. (2009). The importance of myocardial amino acids during ischemia and reperfusion in dilated left ventricle of patients with degenerative mitral valve disease. *Mol. Cell. Biochem.* 330 (1–2), 63–70. doi:10.1007/s11010-009-0101-x

Williams, N. C., and O'Neill, L. A. J. (2018). A role for the Krebs cycle intermediate citrate in metabolic reprogramming in innate immunity and inflammation. *Front. Immunol.* 9, 141. doi:10.3389/fimmu.2018.00141

Wu, X., Song, M., Qiu, P., Li, F., Wang, M., Zheng, J., et al. (2018). A metabolite of nobiletin, 4′-demethylnobiletin and atorvastatin synergistically inhibits human colon cancer cell growth by inducing G0/G1 cell cycle arrest and apoptosis. *Food & Funct.* 9 (1), 87–95. doi:10.1039/C7FO01155E

Xiao, G., Liu, J., Wang, H., He, S., Liu, J., Fan, G., et al. (2022). CXCR1 and its downstream NF-κB inflammation signaling pathway as a key target of Guanxinning injection for myocardial ischemia/reperfusion injury. *Front. Immunol.* 13, 1007341. doi:10.3389/fimmu.2022.1007341

Xu, J., Pan, H., Xie, X., Zhang, J., Wang, Y., and Yang, G. (2018). Inhibiting succinate dehydrogenase by dimethyl malonate alleviates brain damage in a rat model of cardiac arrest. *Neuroscience* 393, 24–32. doi:10.1016/j.neuroscience.2018.09.041

Xu, X.-N., Jiang, Y., Yan, L. Y., Yin, S. Y., Wang, Y. H., Wang, S. B., et al. (2021). Aesculin suppresses the NLRP3 inflammasome-mediated pyroptosis via the Akt/GSK3β/NF-κB pathway to mitigate myocardial ischemia/reperfusion injury. *Phytomedicine Int. J. phytotherapy Phytopharm.* 92, 153687. doi:10.1016/j.phymed.2021.153687

Yamamoto, T., Byun, J., Zhai, P., Lkeda, Y., Oka, S., et al. (2014). Nicotinamide mononucleotide, an intermediate of NAD+ synthesis, protects the heart from ischemia and reperfusion. *PLoS ONE* 9 (6), e98972. doi:10.1371/journal.pone.0098972

Yang, Y., and Sauve, A. A. (2016). NAD + metabolism: Bioenergetics, signaling and manipulation for therapy. *Biochimica Biophysica Acta (BBA) - Proteins Proteomics* 1864 (12), 1787–1800. doi:10.1016/j.bbapap.2016.06.014

Yi, X., Jiang, X., Li, X., and Jiang, D. S. (2017). Histone lysine methylation and congenital heart disease: From bench to bedside (Review). *Int. J. Mol. Med.* 40 (4), 953–964. doi:10.3892/ijmm.2017.3115

Yokoyama, S., Nakagawa, I., Ogawa, Y., Morisaki, Y., Motoyama, Y., Park, Y. S., et al. (2019). Ischemic postconditioning prevents surge of presynaptic glutamate release by activating mitochondrial ATP-dependent potassium channels in the mouse hippocampus. *PloS One* 14 (4), e0215104. doi:10.1371/journal.pone.0215104

Zhang, W., Qiaobing, H., Zhenhua, Z., Jie, W., Yaoyuan, Z., Zhongqing, C., et al. (2017) Sirt1 inhibits oxidative stress in vascular endothelial cells.', *Oxidative Med. Cell. Longev.* 7543973. doi:10.1155/2017/7543973

Zhang, Y., Yu, W., Han, D., Meng, J., Wang, H., and Cao, G. (2019). L–lysine ameliorates sepsis-induced acute lung injury in a lipopolysaccharide-induced mouse model. *Biomed. Pharmacother.* 118, 109307. doi:10.1016/j.biopha.2019.109307

Zuurbier, C. J., Bertrand, L., Beauloye, C. R., Andreadou, I., Ruiz-Meana, M., Jespersen, N. R., et al. (2020). Cardiac metabolism as a driver and therapeutic target of myocardial infarction. *J. Cell. Mol. Med.* 24 (11), 5937–5954. doi:10.1111/jcmm.15180